

## Histidine Residues in the Peptide D-Lys<sup>6</sup>-GnRH: Potential for Copolymerization in Polymeric Nanoparticles

Alexandra P. Kafka,<sup>†</sup> Torsten Kleffmann,<sup>‡</sup> Thomas Rades,<sup>†</sup> and  
Arlene McDowell<sup>\*,†</sup>

School of Pharmacy, University of Otago, Dunedin 9054, New Zealand, and Centre for Protein  
Research, Department of Biochemistry, University of Otago, Dunedin 9054, New Zealand

Received February 4, 2009; Revised Manuscript Received May 15, 2009; Accepted August 5, 2009

**Abstract:** Poly(ethylcyanoacrylate) (PECA) nanoparticles containing the bioactive D-Lys<sup>6</sup>-GnRH were manufactured by an *in situ* interfacial polymerization process using a w/o-microemulsion template containing the peptide in the dispersed aqueous pseudophase of the microemulsion. Polymeric nanoparticles were characterized using PCS, RP-HPLC (bulk level) and MALDI TOF mass spectrometry (molecular level). The peptide D-Lys<sup>6</sup>-GnRH was reactive with the alkylcyanoacrylate monomer, resulting in some of the peptide copolymerizing with the monomer. MALDI TOF/TOF (tandem) analysis revealed that the histidine residue in position 2 of D-Lys<sup>6</sup>-GnRH interacts covalently in the polymerization process. A reaction mechanism for this nucleophilic interference is suggested. The copolymerization reaction appeared to occur within seconds after the addition of the monomer to the microemulsion. The surface charge of resulting nanoparticles was less negative (−3 mV) compared with the zeta potential of empty nanoparticles (−27.5 mV). The copolymerization yielded high entrapment rates of 95 ± 4% of peptide, but showed limited release (~11%) of free peptide over 5 days. A separate experiment demonstrated that the addition of D-Lys<sup>6</sup>-GnRH to preformed empty PECA nanoparticles (*ex situ*) also yielded fractions of copolymerized peptide suggesting a certain proportion of polymer remains available for copolymerization possibly through an unzipping depolymerization/repolymerization process. Therefore, the reactivity of histidine residues in bioactives needs to be considered whenever using the bioactive *in situ* or *ex situ* with polymeric PECA nanoparticles.

**Keywords:** Poly(alkylcyanoacrylate); D-Lys<sup>6</sup>-GnRH; MALDI TOF; copolymerization; histidine

### 1. Introduction

Nanoparticulate delivery systems, particularly poly(alkylcyanoacrylate) (PACA) nanoparticles, have been investigated for several decades, and comprehensive reviews are available on their biomedical applications as controlled drug delivery systems.<sup>1–4</sup> PACA nanoparticles, including nanospheres and nanocapsules, can be prepared using various techniques.<sup>1,4</sup>

The anionic interfacial polymerization technique of producing nanocapsules has a number of advantages, including high entrapment efficiencies (~85%) of high molecular weight bioactives, such as insulin<sup>5,6</sup> and calcitonin.<sup>7</sup> Using w/o-microemulsions as polymerization templates is especially beneficial for PACA formulations with peroral applications since the templates are biodegradable and biocompatible<sup>8</sup> and exhibit permeation enhancing properties.<sup>9</sup> Furthermore, using microemulsions as polymerization templates is advan-

\* Corresponding author: Dr. Arlene McDowell, University of Otago, School of Pharmacy, 18 Frederick Street, PO Box 56, 9054 Dunedin, New Zealand. E-mail: arlene.mcdowell@otago.ac.nz. Phone: +64 3 479 7145. Fax: + 64 3 479 703.

<sup>†</sup> School of Pharmacy.

<sup>‡</sup> Centre for Protein Research, Department of Biochemistry.

(1) Vauthier, C.; Dubernet, C.; Fattal, E.; Pinto-Alphandary, H.; Couvreur, P. Poly(alkylcyanoacrylates) as biodegradable materials for biomedical applications. *Adv. Drug Delivery Rev.* **2003**, *55*, 519–548.

(2) Allemann, E.; Leroux, J. C.; Gurny, R. Polymeric nano- and microparticles for the oral delivery of peptides and peptidomimetics. *Adv. Drug Delivery Rev.* **1998**, *34*, 171–189.

(3) des Rieux, A.; Fievez, V.; Garinot, M.; Schneider, Y. J.; Preat, V. Nanoparticles as potential oral delivery systems of proteins and vaccines: A mechanistic approach. *J. Controlled Release* **2006**, *116*, 1–27.

tageous since no high energy input is necessary for their production.<sup>5,10</sup>

Anionic interfacial polymerization is usually initiated by the hydroxyl ions arising from the autoprotolysis of water, although other weak bases such as alcohols and amino acids may also function as initiators.<sup>1</sup> For example, our group has prepared poly(ethylcyanoacrylate) (PECA) nanoparticles using a water-free microemulsion where propylene glycol served as the reaction initiator.<sup>11</sup> The polymerization reaction is considered to happen rapidly within seconds or minutes. Urlaub et al.<sup>12</sup> monitored the polymerization reaction of different alkylcyanoacrylate monomers both on a bulk level and in single trapped microparticles using Raman microscopy. The polymerization kinetics of a drop of ethylcyanoacrylate exposed to air was found to be fast (400 s), whereas the reaction kinetics of PECA microparticles in an emulsion was too fast to be detected.

Simultaneous to polymer formation, polymer degradation may occur through various mechanisms. *In vitro* degradation has been suggested to occur via two mechanisms. The first mechanism takes place in water and involves an inversed Knoevenagel reaction yielding formaldehyde and alkyl cyanoacetate. Leonard et al.<sup>13</sup> found approximately 5% of polymer degraded within 24 h with the resulting formaldehyde considered to be responsible for the adverse effects of PACA polymers when used for biomedical applications. More recently, the occurrence of formaldehyde during the

early stages of polymer formation has been demonstrated by Bootz et al.<sup>14</sup> A second degradation mechanism also suggested to take place during the early stages of polymer formation involves the base-catalyzed unzipping depolymerization and immediate repolymerization of polymers.<sup>15</sup> The parent polymer is unzipped to yield intermediate states of reactive anionic species, including monomers, oligomers or “daughter polymers”. The repolymerization of these species occurs within seconds, resulting in lower molecular weight polymers compared to parent polymer.<sup>15</sup>

*In situ* polymerization requires both the monomer and the drug to be present during the polymerization process. Thus drug can potentially interfere with the (re)polymerization process. Incomplete release (<80%) of drugs from PACA nanoparticles produced by *in situ* polymerization has been observed, and copolymerization has been suggested as the reason.<sup>16,17</sup>

Tandem mass spectrometry is particularly suitable for the molecular characterization of certain nanoparticulate delivery systems and the mechanism of interaction and entrapment of bioactives. Accurate mass measurement, in combination with the analysis of fragmentation characteristics using collision induced dissociation (CID) mass spectrometry (MS), allows unambiguous identification of covalent interaction sites between polymer and bioactives. Unraveling the mechanisms of bioactive–polymer interaction helps to explain entrapment and release characteristics of the resulting nanoparticles.

Gonadotropin releasing hormone (GnRH, pGlu-His-Trp-Ser-Tyr-Gly<sup>6</sup>-Leu-Arg-Pro-GlyNH<sub>2</sub>) is the master hormone of the reproductive system and regulates the secretion of luteinizing hormone and follicle stimulating hormone.<sup>18</sup> GnRH and its analogues have applications in cancer therapy<sup>12</sup> and are also considered potential candidates for future fertility control strategies in wild animals.<sup>19,20</sup> In this study we used

- (4) Couvreur, P.; Barratt, G.; Fattal, E.; Legrand, P.; Vauthier, C. Nanocapsule technology: A review. *Crit. Rev. Ther. Drug Carrier Syst.* **2002**, *19*, 99–134.
- (5) Watnasirichaikul, S.; Davies, N. M.; Rades, T.; Tucker, I. G. Preparation of biodegradable insulin nanocapsules from biocompatible microemulsions. *Pharm. Res.* **2000**, *17*, 684–689.
- (6) Dange, C.; Vranckx, H.; Balschmidt, P.; Couvreur, P. Poly(alkyl cyanoacrylate) nanospheres for oral administration of insulin. *J. Pharm. Sci.* **1997**, *86*, 1403–1409.
- (7) Lowe, P. J.; Temple, C. S. Calcitonin and Insulin in Isobutylcyanoacrylate Nanocapsules - Protection against Proteases and Effect on Intestinal-Absorption in Rats. *J. Pharm. Pharmacol.* **1994**, *46*, 547–552.
- (8) Watnasirichaikul, S.; Rades, T.; Tucker, I. G.; Davies, N. M. Effects of formulation variables on characteristics of poly (ethylcyanoacrylate) nanocapsules prepared from w/o microemulsions. *Int. J. Pharm.* **2002a**, *235*, 237–246.
- (9) Constantinides, P. P.; Lancaster, C. M.; Marcello, J.; Chiossone, D. C.; Orner, D.; Hidalgo, I.; Smith, P. L.; Sarkahian, A. B.; Yiv, S. H.; Owen, A. J. Enhanced Intestinal-Absorption of an Rgd Peptide from Water-in-Oil Microemulsions of Different Composition and Particle-Size. *J. Controlled Release* **1995**, *34*, 109–116.
- (10) Couvreur, P.; Dubernet, C.; Puisieux, F. Controlled Drug-Delivery with Nanoparticles - Current Possibilities and Future-Trends. *Eur. J. Pharm. Biopharm.* **1995**, *41*, 2–13.
- (11) Krauel, K.; Graf, A.; Hook, S. M.; Davies, N. M.; Rades, T. Preparation of poly (alkylcyanoacrylate) nanoparticles by polymerization of water-free microemulsions. *J. Microencapsulation* **2006**, *23*, 499–512.
- (12) Anderson, J.; Abrahamsson, P. A.; Crawford, D.; Miller, K.; Tombal, B. Management of advanced prostate cancer: can we improve on androgen deprivation therapy. *BJU Int.* **2008**, *101*, 1497–1501.
- (13) Leonard, F.; Kulkarni, R. K.; Brandes, G.; Nelson, J.; Cameron, J. J. Synthesis and Degradation of Poly(Alkyl Alpha-Cyanoacrylates). *J. Appl. Polym. Sci.* **1966**, *10*, 259. ff.
- (14) Bootz, A.; Russ, T.; Gores, F.; Karas, M.; Kreuter, J. Molecular weights of poly(butyl cyanoacrylate) nanoparticles determined by mass spectrometry and size exclusion chromatography. *Eur. J. Pharm. Biopharm.* **2005**, *60*, 391–399.
- (15) Ryan, B.; McCann, G. Novel sub-ceiling temperature rapid depolymerization-repolymerization reactions of cyanoacrylate polymers. *Macromol. Rapid Commun.* **1996**, *17*, 217–227.
- (16) Pitaksutepong, T.; Davies, N. M.; Tucker, I. G.; Rades, T. Factors influencing the entrapment of hydrophilic compounds in nanocapsules prepared by interfacial polymerisation of water-in-oil microemulsions. *Eur. J. Pharm. Biopharm.* **2002**, *53*, 335–342.
- (17) Fawaz, F.; Guyot, M.; Lagueny, A. M.; Devissaguet, J. P. Ciprofloxacin-loaded polyisobutylcyanoacrylate nanoparticles: preparation and characterization. *Int. J. Pharm.* **1997**, *154*, 191–203.
- (18) Padula, A. M. GnRH analogues—agonists and antagonists. *Anim. Reprod. Sci.* **2005**, *88*, 115–126.
- (19) Schultze-Mosgau, A.; Griesinger, G.; Altgassen, C.; von Otte, S.; Hornung, D.; Diedrich, K. New developments in the use of peptide gonadotropin-releasing hormone antagonists versus agonists. *Expert Opin. Invest. Drugs* **2005**, *14*, 1085–1097.

the GnRH analogue D-Lys<sup>6</sup>-GnRH (p-Glu-His-Trp-Ser-Tyr-Lys<sup>6</sup>-Leu-Arg-Pro-GlyNH<sub>2</sub>), which is part of a project investigating fertility control of pest species in New Zealand using oral delivery strategies.<sup>21</sup>

The aim of this study was to prepare and characterize PECA nanoparticles containing the bioactive D-Lys<sup>6</sup>-GnRH using the interfacial polymerization technique and to use MALDI TOF/TOF MS to gain more detailed insight into this copolymerized PECA delivery system on a molecular level. Copolymer formation with peptide during the *in situ* polymerization process was compared to the *ex situ* addition of peptide to polymer nanoparticles prepared in the absence of peptide. A plausible mechanism for the bioactive–polymer interaction observed is also suggested.

## 2. Experimental Section

**2.1. Reagents.** The GnRH analogue, D-Lys<sup>6</sup>-GnRH (p-Glu-His-Trp-Ser-Tyr-Lys<sup>6</sup>-Leu-Arg-Pro-GlyNH<sub>2</sub>), was purchased from PolyPeptide Laboratories (Torrance, CA). For preparation of microemulsions, the oil component ethyl oleate GPR was sourced from BDH Laboratory Supplies (Poole, England) and the surfactants sorbitan monolaurate (Crill 1) and ethoxy 20 sorbitan mono-oleate (Crillet 4) were kindly provided by BTB Chemicals (Auckland, New Zealand). The monomer ethylcyanoacrylate (ECA) (Sicomet 40) was kindly donated by Henkel Loctite (Hannover, Germany). Methanol (HPLC grade), chloroform and hydrochloric acid (fuming 37%, GR for analysis) were obtained from Merck KGaA (Darmstadt, Germany). Ethanol was supplied by AnchorEthanol (Auckland, New Zealand). Phosphate buffer pH 7.4 was prepared by mixing 0.1 M solutions of potassium dihydrogenorthophosphate and disodium hydrogenorthophosphate (both from BDH Laboratory Supplies, Poole, England) at a ratio of 10:81. Sodium chloride was obtained from Univar, Asia Pacific Specialty Chemicals Limited (Sydney, Australia). For HPLC analysis, trifluoroacetic acid (TFA) was sourced from Sigma-Aldrich (St. Louis, MO) and acetonitrile (HPLC grade) was purchased from Merck KGaA (Darmstadt, Germany). Distilled, ultrapure water was obtained from a Milli-Q water Millipore Purification System (USA) and was used at all times during HPLC analysis and sample preparation.

**2.2. Preparation of PECA Nanoparticles from a Microemulsion Template.** The microemulsion template was prepared based on the method of Watnasirichaikul et al.<sup>22</sup> In short, the surfactants Crill 1 and Crillet 4 were mixed in a

4:6 weight ratio. To obtain a microemulsion, water, oil and surfactant-blend were mixed together at a 1:3.6:5.4 weight ratio. For preparation of drug loaded particles, the GnRH analogue was dissolved in the water phase (8 mg/mL) prior to mixing with the other ingredients. Microemulsion formation occurred instantly upon stirring at 700 rpm at 4 °C. Ten grams of microemulsion was polymerized with 200 µL of ECA monomer dissolved in 600 µL of chloroform. The monomer was added dropwise to the microemulsion template under continuous stirring at 700 rpm at 4 °C. Samples were withdrawn at certain time points during the polymerization process and analyzed with MALDI MS. After the addition of monomer, the mixture was left overnight to complete the interfacial polymerization process and to evaporate the chloroform. Resulting nanocapsules were characterized the following day.

**2.3. Characterization of PECA Nanoparticles.** **2.3.1. Size and Zeta Potential Measurement.** The size and zeta potential of isolated nanoparticles were determined using photon correlation spectroscopy (Zetasizer 3000, Malvern Instruments Ltd., U.K.). Nanoparticles were mixed with 600 µL of Milli-Q water pH 2.5 (pH adjusted with hydrochloric acid) and 600 µL of methanol 80% (v/v, water pH 2.5) and separated from the surrounding microemulsion by centrifugation at 20800g and 25 °C for 20 min (Eppendorf Centrifuge 5417C). Nanoparticles were washed in ethanol (abs.) twice to remove residual oil and surfactants. The nanoparticles used for size measurements were redispersed in ethanol (abs.) containing 0.2% (w/v) polysorbate 80,<sup>5</sup> and nanoparticles for zeta potential measurement were resuspended in 1 mM NaCl solution. Size and zeta potential were measured at room temperature.

**2.3.2. Entrapment Efficiency.** Entrapment efficiency was determined as the difference between the amount of peptide added to the formulation prior to polymerization and the amount recovered from the supernatant after polymerization. 0.5 g of microemulsion containing nanoparticles was mixed with 3 mL of Milli-Q water pH 2.5 (pH adjusted with 3% HCl solution). An aliquot of 600 µL was mixed with 600 µL of methanol 80% (v/v, water pH 2.5). The oil and water phase in this mixture were separated by centrifugation at 20800g (Eppendorf Centrifuge 5417C, *t* = 20 min, *T* = 25 °C). Peptide in the aqueous phase was analyzed by gradient RP-HPLC.

**2.3.3. Release Study.** Release was studied at a pH of 7.4 to mimic the drug release after absorption from the oral route or after direct systemic administration. Due to the instability of D-Lys<sup>6</sup>-GnRH in the presence of microemulsion and phosphate buffer compounds at pH 7.4,<sup>23</sup> the release characteristics of PECA nanoparticles were studied in water pH 7.4 (adjusted with NaOH solution) in order to investigate the maximum amount potentially released. Two grams of

(20) Herbert, C. A.; Trigg, T. E. Applications of GnRH in the control and management of fertility in female animals. *Anim. Reprod. Sci.* **2005**, *88*, 141–153.

(21) McDowell, A.; McLeod, B. J.; Rades, T.; Tucker, I. G. Application of pharmaceutical drug delivery for biological control of the common brushtail possum in New Zealand: a review. *Wildl. Res.* **2006**, *33*, 679–689.

(22) Guzman, N. A. Determination of immunoreactive gonadotropin-releasing hormone in serum and urine by on-line immunoaffinity capillary electrophoresis coupled to mass spectrometry. *J. Chromatogr. B* **2000**, *749*, 197–213.

(23) Kafka A. P.; Rades T.; McDowell A. Rapid and specific high-performance liquid chromatography for the *in vitro* quantification of D-Lys<sup>6</sup>-GnRH in a microemulsion-type formulation in the presence of peptide oxidation products. *Biomed. Chromatogr.* DOI: 0.1002/bmc.1261.



formulation was mixed with 15 mL of release medium and then transferred into a double-walled thermostated beaker at 37 °C under continuous stirring at 400 rpm for 5 days. 400  $\mu$ L of sample was withdrawn at specific time points and mixed with 400  $\mu$ L of methanol 80% (v/v, water pH 2.5). The samples were centrifuged at 20800g (Eppendorf Centrifuge 5417C,  $t$  = 20 min,  $T$  = 25 °C) to separate the oil and water phase. The peptide content was quantified in the clear aqueous phase by gradient RP-HPLC.

**2.4. Peptide Adsorption onto Preformed PECA Nanoparticles.** Empty PECA nanoparticles were polymerized in the absence of peptide as above and stirred for 4 h at 4 °C, since the polymerization reaction has been reported to be complete after 4 h.<sup>5</sup> Eight milligrams of D-Lys<sup>6</sup>-GnRH dissolved in 200  $\mu$ L water was added to the polymerized microemulsion. The formulation was kept at 4 °C and stirred at 700 rpm. After the addition of peptide, samples were withdrawn after 0.5 h, 4 h and 4 days, mixed with reaction termination medium (aqueous TFA, pH 1.9) and an equal volume of methanol 80% (v/v, water pH 2.5). The mixture was centrifuged at 20800g (Eppendorf Centrifuge 5417C,  $t$  = 20 min,  $T$  = 25 °C) to separate the polymer pellet from oil and water phase. The peptide content was quantified in the clear aqueous phase by gradient RP-HPLC. The polymeric nanoparticles were washed twice in ethanol (abs.), then either dissolved in acetonitrile for mass spectrometric analysis or redispersed in 1 mM NaCl solution for determination of zeta potential according to section 2.3.1.

**2.5. RP-HPLC Analysis.** Gradient RP-HPLC analysis was carried out using an Agilent series 1200 HPLC system (Santa Clara, CA) equipped with quaternary pump and micro vacuum degasser (G 1379B). Samples were kept at 4 °C in a thermostated autosampler (G 1329A with a G 1330B thermostat), and the column compartment (G 1316A) was maintained at 40 °C. All samples were measured at 220 nm using a variable wavelength detector (G 1314 B). Sample aliquots of 50  $\mu$ L were loaded in 90% of solvent A (0.1% TFA in Milli-Q water) onto a Jupiter C18 column (250  $\times$  4.6 mm i.d., 5  $\mu$ m particle size, 300 Å, Phenomenex, Torrance, CA) protected by a C18 Phenomenex Analytical Guard cartridge column (KJ0-4282, 4.0 L mm  $\times$  3.0 i.d. mm) at a flow rate of 1 mL/min. Samples were eluted by a gradient developed from 10 to 35% of solvent B (0.1% TFA in CH<sub>3</sub>CN) in solvent A (0.1% TFA in Milli-Q water) at a flow rate of 1 mL/min over 12 min. In a second step, the concentration of solvent B was increased to 90% over an additional 3 min at a flow rate of 1.2 mL/min to remove other formulation components such as oil and surfactants. To re-equilibrate the system, the concentration of solvent B was decreased to 10% over a period of 5 min, followed by another 10 min at a reduced flow rate of 1 mL/min. Peptide quantification as for sections 2.3.2, 2.3.3, and 2.4 was carried out using a standard curve (range 7.5 to 60  $\mu$ g/mL). For details on the validation procedure of the HPLC method, we refer to Kafka et al.<sup>23</sup> The method was linear over the concentration range 2.5 to 60  $\mu$ g/mL.<sup>23</sup> Lower limits of

detection (LLOD) and lower limit of quantification (LLOQ) were determined to be 0.13  $\mu$ g/mL and 0.38  $\mu$ g/mL respectively.<sup>23</sup>

**2.6. MALDI TOF Mass Spectrometry.** Washed nanoparticles to be analyzed by matrix-assisted laser desorption/ionization tandem time-of-flight (MALDI TOF/TOF) mass spectrometry were dissolved in approximately 20–40  $\mu$ L of acetonitrile. 1.0  $\mu$ L of sample solution was mixed with 9.0  $\mu$ L of matrix (10 mg/mL alpha cyano-4-hydroxycinnamic acid dissolved in 60% (v/v) aqueous acetonitrile containing 0.1% (v/v) TFA). An aliquot of 0.8  $\mu$ L was spotted onto the MALDI-plate (Opti-TOF 384 well plate, Applied Biosystems, Framingham, MA) and air-dried. Samples were analyzed on a 4800 MALDI tandem Time-of-Flight Analyzer (Applied Biosystems, Framingham, MA). The default calibration for each operation mode was updated on six calibration spots. All MS spectra were acquired in positive-ion reflector mode with 1000 laser pulses per sample spot.

Precursor ions of interest were selected for collision induced dissociation tandem mass spectrometry (CID-MS/MS). CID-MS/MS spectra were acquired with 2000–4000 laser pulses per selected precursor using the 2 kV mode and air as the collision gas at a pressure of  $1 \times 10^{-6}$  Torr. CID-MS/MS spectra were interpreted manually. Only b-, y- and a-type ions as well as relevant immonium ions were considered and annotated according to the Biemann nomenclature.<sup>24</sup> Briefly, CID of a selected peptide species in the collision cell of a mass spectrometer generates sequence specific product ions (fragment ions), which are detected and recorded in a CID-MS/MS spectrum. Positive ion mode low energy CID based peptide cleavage at peptide bonds yields potentially two types of product ions, one carrying the N-terminus and the other carrying the C-terminus, which are referred to as b-type ions and y-type ions respectively. An additional loss of carbon monoxide from b-type ions under conditions of low energy CID results in a-type ions which are always 28 mass units apart from the respective b-ions. Immonium ions are low mass product ions generated by multiple cleavage events and represent a single amino acid side chain still bound to the  $\alpha$  carbon with the  $\alpha$  amino group attached. Immonium ions are labeled with the single letter code of the respective amino acid and are indicative for the presence of certain amino acids in the peptide. However they do not reveal the position of the amino acids in the sequence. The sequence of amino acids is determined by a series of consecutive b-ions with b<sub>1</sub> being the N-terminal amino acid or y-ions with y<sub>1</sub> being the C-terminal amino acid. Both ion series extend from the termini by increments according to the masses of following internal amino acids and are labeled with the type of ion and ascending subscript numbers. An amino acid modification can be identified by a specific shift of one or a group of related ions in the CID MS/MS spectrum relative to the expected masses.

(24) Biemann, K. Nomenclature for Peptide Fragment Ions (Positive-Ions). *Methods Enzymol.* **1990**, *193*, 886–887.

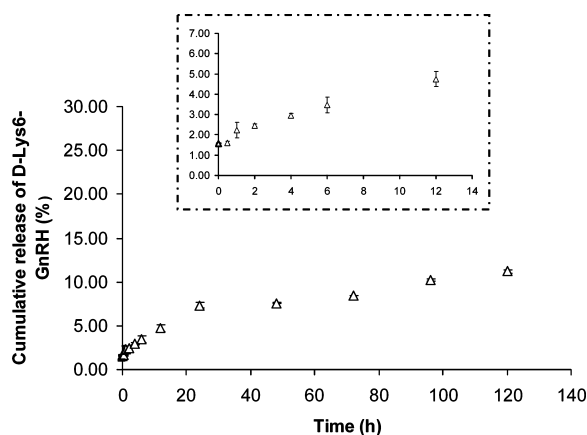


**Figure 1.** Cumulative release of D-Lys<sup>6</sup>-GnRH from nanoparticles (Δ) monitored over 5 days. Values represent means  $\pm$  SD ( $n$  number of repetitions = 3). Inset shows the release over the first 12 h. Release medium was Milli-Q water pH 7.4 (adjusted with 0.1 M NaOH).

**2.7. Statistical Analysis.** The differences in mean nanoparticle size for formulations containing the peptide and blank formulations and differences in zeta potential for blank PECA nanoparticles and nanoparticles following the adsorption experiment were tested by a Student's  $t$  test using Microsoft Excel (Version 2003).  $P$ -Values  $< 0.05$  were considered to be significant.

### 3. Results

**3.1. Characterization of Nanoparticles.** The mean size of D-Lys<sup>6</sup>-GnRH-containing PECA nanoparticles was  $188 \pm 13$  nm and  $194 \pm 24$  nm for the unloaded nanoparticles. Mean sizes were not significantly different ( $P > 0.05$ ). The polydispersity index was low for both the loaded ( $0.105 \pm 0.048$ ) and the unloaded nanoparticles ( $0.126 \pm 0.040$ ), indicating a narrow size distribution. The zeta potential was less negative ( $-3$  mV) when polymerized in the presence of D-Lys<sup>6</sup>-GnRH compared to empty particles ( $-27.5$  mV). Entrapment efficiency of D-Lys<sup>6</sup>-GnRH in PECA nanoparticles was  $95 \pm 4\%$ .

**3.2. Release Study.** The overall cumulative release of D-Lys<sup>6</sup>-GnRH from PECA nanoparticles after 5 days of study in water pH 7.4 was low (11%). No burst release was observed. The amount of D-Lys<sup>6</sup>-GnRH detected at  $t = 0$  h is consistent with the amount of untrapped peptide ( $1.58 \pm 0.02\%$ ). Following an initial short lag phase of approximately 0.5 h (insert Figure 1), approximately 7% of the drug was released after 24 h of release (Figure 1). Between 24 and 48 h, the release profile shows a plateau with minimal amount of peptide being released. After 48 h, another slower release onset can be observed and a further 4% of the peptide is released slowly over the following 3 days (Figure 1).

MALDI TOF mass spectrometry revealed a proportion of the D-Lys<sup>6</sup>-GnRH peptide to be covalently associated with oligomer subunits of PECA nanoparticles. Mass spectra of unloaded PECA nanoparticles dissolved in acetonitrile

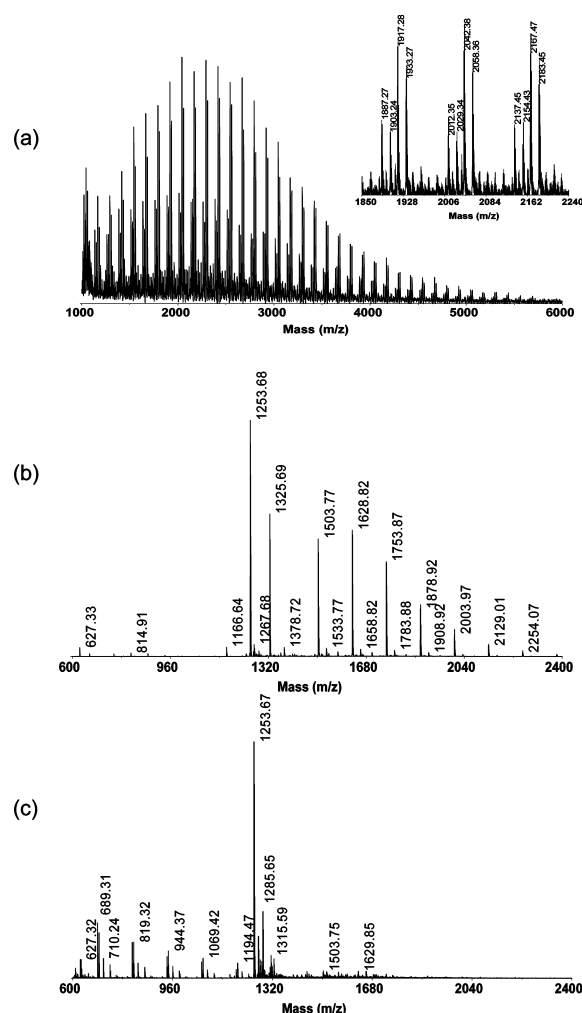


**Figure 2.** Mass spectra of PECA nanoparticles: (a) unloaded PECA nanoparticles, (b) polymerized PECA nanoparticles in the presence of D-Lys<sup>6</sup>-GnRH before and (c) after the 5 days of release. Free peptide is visible at  $[M + H]^+$  at  $m/z$  1253.6 and peptide/ECA copolymers  $[M + (125)_n + H]^+$  at  $m/z$  1378.7, 1503.8, 1628.8, 1753.9, 1878.9, 2003.0 etc.

showed characteristic peak increments of 125 mass units, which correlate with the sequential addition of monomer subunits (Figure 2(a)). Mass spectra of polymerized peptide-loaded nanoparticles (Figure 2(b)) showed a peak  $[M + H]^+$  for the free peptide at  $m/z$  1253.6 as well as peaks of peptide copolymerized with ECA-subunits indicated by mass shifts of 125 relative to the free peptide  $[M + (125)_n + H]^+$ . Copolymer chains of peptide associated with 2–4 ECA subunits showed the highest peak intensities ( $m/z$  1503.8, 1628.8 and 1753.8) (Figure 2(b)). Non-peptide-associated polymer was only observed as low intensity peaks in the low mass range ( $m/z$  600–1200) of the spectrum (Figure 2(b)). Mass spectra of dissolved PECA polymer obtained from samples taken at earlier stages during the polymerization process (starting after 15 s) were not different from the mass spectrum in Figure 2(b), which was obtained 12 h post-polymerization (data not shown). In contrast, after release

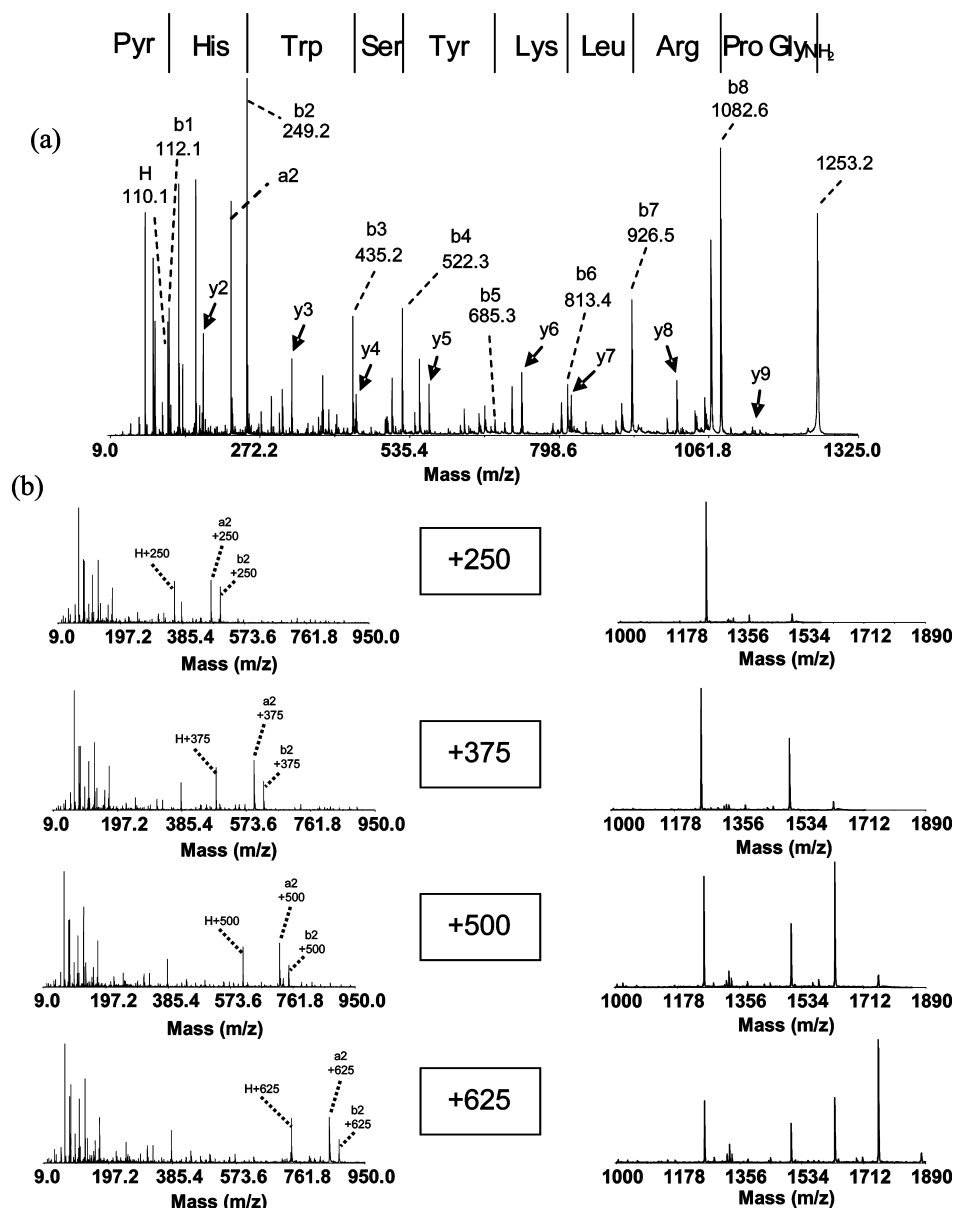


**Figure 3.** MALDI TOF MS/MS spectra of (a) the parent peptide D-Lys<sup>6</sup>-GnRH ( $m/z$  1253.2), fragments aligned with the amino acid sequence of the D-Lys<sup>6</sup>-GnRH and (b) a sequence of four precursor ions of the copolymerized peptide (top to bottom  $m/z$  1503.8, 1628.8, 1753.8 and 1878.8); b1–b8 fragments carry the N-terminus, y2–y9 fragments carry the C-terminus of the D-Lys<sup>6</sup>-GnRH. Left: enlargement of the low molecular mass range; the diagnostic b<sub>2</sub> and a<sub>2</sub>-fragment ions, and the immonium histidine ion (H) are indicated and shifted by mass units of (125)<sub>n</sub> with *n* referring to the number of monomer subunits copolymerized (top to bottom 2,3,4,5). Right: enlargement of the higher molecular mass range and showing fragmentation of the precursor ions with increments of  $m/z$  125; precursor  $m/z$  1503.8 shows fragment signals at  $m/z$  1378.8 and 1253.6, precursor 1628.8 at  $m/z$  1503.8, 1378.8 and 1253.7, precursor 1753.8 at  $m/z$  1628.8, 1503.8, 1378.8, and 1253.6 etc.

for 5 days (Figure 2(c)), the mass spectrum showed free peptide ( $m/z$  1253.6) as well as non-peptide-associated polymer ( $m/z$  819.32, 944.37, 1069.42), indicating a certain degree of degradation of the copolymer during the release study.

**3.3. Characterization of the Peptide/ECA Covalent Interaction by CID MS/MS.** To identify the site and mechanism of D-Lys<sup>6</sup>-GnRH/ECA copolymerization, the CID fragment spectrum of the precursor  $m/z$  1253.6 (free D-Lys<sup>6</sup>-GnRH) was compared with CID spectra of the precursor ions  $m/z$  1503.8, 1628.8, 1753.8, and 1878.8 of the D-Lys<sup>6</sup>-GnRH/

ECA copolymers. The fragmentation of the precursor ion  $m/z$  1253.6 by CID MS/MS revealed complete amino acid sequence information of D-Lys<sup>6</sup>-GnRH by a comprehensive series of b-ions and y-ions with the only missing peaks being b<sub>9</sub> and y<sub>1</sub> of the C-terminal amidated glycine (Figure 3(a)). In the CID spectra of peptide/ECA copolymers all b-ions from position 2 and higher were shifted by a multiple of 125 according to the number of attached ECA subunits (Figure 3(b)), while the b<sub>1</sub> ion and the y<sub>2</sub>–y<sub>8</sub> ions were consistent in all spectra. The characteristic shift of a multiple

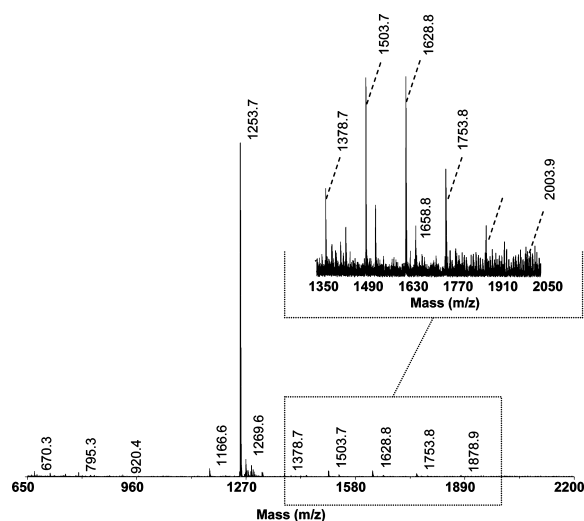


**Figure 4.** MALDI TOF mass spectra of PECA nanoparticles 4 h after D-Lys<sup>6</sup>-GnRH (8 mg/mL) was added *ex situ*. Inset on the right enlarges the range  $m/z$  1350 to 2050 clearly showing the presence of peptide/ECA copolymers  $[M + (125)_{1-6} + H]^+$  at  $m/z$  1378.7, 1503.7, 1628.8, 1753.8, 1878.9, and 2003.9; free D-Lys<sup>6</sup>-GnRH peptide at  $m/z$  1253.6.

of 125 from b2 and higher identifies the site of modification occurs at position 2. Moreover, the diagnostic low mass ion for the single histidine side chain (histidine immonium ion) at  $m/z$  110.1 is also shifted by a multiple of 125, confirming the ECA subunit resides at the His2 side chain.

**3.4. Peptide Adsorption onto Preformed PECA Nanoparticles.** After adding 8 mg of peptide *ex situ* to empty preformed PECA nanoparticles, peptide/ECA copolymers occur after 4 h of incubation (4 °C, stirred at 700 rpm) as detected by MALDI TOF mass spectrometry (Figure 4). Peptide associated with 2 and 3 monomer subunits  $[M + (125 \text{ Da})_{2,3} + H]^+$  with  $m/z$  1503.8 and 1628.8 had the strongest peak intensities of all copolymers (Figure 4). The maximum mass  $[M + (125)_7 + H]^+$  of 2129.1 detectable in our experiments corresponds to peptide + 7 ECA subunits. After 4 days of study, slightly longer copolymers with up to 9 ECA subunits were detected. When analyzing the supernatants using RP-HPLC analysis, approximately 84% of the initially added amount of peptide was recovered from an unpolymerized microemulsion and 75% after 4 h of incubation in the presence of preformed polymeric nanoparticles. This suggests approximately 9% of the peptide is associated with the nanoparticle via adsorption and/or copolymerization. However, the zeta potential of the nanoparticles after 0.5 h, 4 h and 4 days of incubation was not significantly different compared to empty PECA nanoparticles before incubation ( $P > 0.05$ ).

## 4. Discussion

The D-Lys<sup>6</sup>-GnRH-loaded PECA nanoparticles produced conform to the usual size of PACA nanoparticles reported in the literature.<sup>1-3,8</sup> The zeta potential changed from  $-27.5$  mV to  $-3$  mV upon peptide loading, suggesting a contribu-

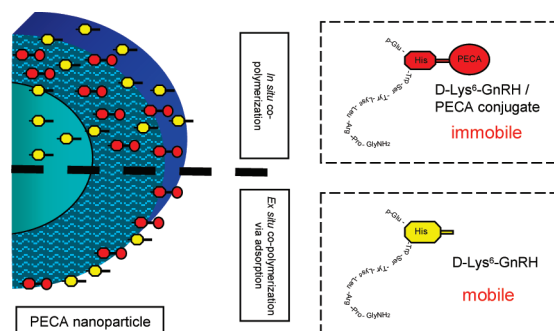


**Figure 5.** Schematic illustration of four potential entrapment mechanisms of D-Lys<sup>6</sup>-GnRH entrapment in PECA nanoparticles; mobile peptide fractions (yellow) may be located in the aqueous core of the nanoparticle, in the wall and in the adsorption layer of the particle; copolymerized peptide/ECA conjugates are considered immobile (red) unless the particles start to degrade.

tion of the peptide (positively charged under measurement conditions, pH 8.5) to the overall net charge of the particle. Contribution may occur upon the adsorption of D-Lys<sup>6</sup>-GnRH onto the particle surface and/or covalent association with polymer. The entrapment efficiency of D-Lys<sup>6</sup>-GnRH in PECA nanoparticles was  $95 \pm 4\%$  and is higher than the entrapment of other compounds of similar or higher molecular weight protein or peptide models such as insulin in PECA nanoparticles ( $\sim 85\%$ )<sup>25</sup> or salmon calcitonin in PBCA (50%).<sup>2,26</sup>

Drug entrapment in PACA nanoparticles has been suggested to occur by four different mechanisms (Figure 5). PACA nanoparticles prepared by the interfacial polymerization of a w/o-microemulsion can entrap hydrophilic drugs within the aqueous core of the particle (1) and within the polymer wall (2).<sup>5</sup> A third fraction may be adsorbed onto the particle surface (3). Adsorption occurs depending on the size and  $pK_a$  of the drug and on the pH of the water compartment in the microemulsion, i.e. the charge status of drug and polymer.<sup>16,27</sup> However, these three drug fractions can be considered mobile as long as the drug is small enough to fit through the polymer network and hence may contribute to the fraction of drug potentially released from the particle, in either an initial burst release (adsorbed fraction) or a secondary release from within the particle core or wall.<sup>16</sup> A fourth, supposedly immobile fraction of drug can be covalently associated with polymer molecules due to copoly-

(25) Watnasirichaikul, S.; Rades, T.; Tucker, I. G.; Davies, N. M. In-vitro release and oral bioactivity of insulin in diabetic rats using nanocapsules dispersed in biocompatible microemulsion. *J. Pharm. Pharmacol.* **2002b**, *54*, 473–480.

(26) Vranckx, H.; Demoustier, M.; Deleers, M. A new nanocapsule formulation with hydrophilic core: Application to the oral administration of salmon calcitonin in rats. *Eur. J. Pharm. Biopharm.* **1996**, *42*, 345–347.

(27) Couvreur, P.; Kante, B.; Roland, M.; Guiot, P.; Bauduin, P.; Speiser, P. Polycyanoacrylate Nanocapsules as Potential Lyso-somotropic Carriers - Preparation, Morphological and Sorptive Properties. *J. Pharm. Pharmacol.* **1979**, *31*, 331–332.



lymerization of drug in the *in situ* polymerization process.<sup>16,17</sup> The total amount of drug entrapped within a particle may be the result of more than one entrapment mechanism (Figure 5).

In our study, the mobile fraction of D-Lys<sup>6</sup>-GnRH in PECA nanoparticles appears to be small. Only 7% of peptide was released over the first 24 h (of the 11% of peptide released in total over 5 days). In contrast, Pitaksuteepong et al.<sup>16</sup> found the cumulative release of FITC-dextran (10 kDa), an approximately 10-fold bigger molecule than D-Lys<sup>6</sup>-GnRH, to increase from an initial burst release of 60% to approximately 80% of the total amount of compound over 6 h. A molecule the size of the D-Lys<sup>6</sup>-GnRH peptide should be released to a much larger extent if entrapped in the mobile drug fraction. MALDI MS of D-Lys<sup>6</sup>-GnRH-loaded particles clearly showed the presence of free peptide, but more interestingly, of peptide copolymerized with ECA subunits indicated by mass adducts of a multiple of 125  $[M + (125)_n + H]^+$  relative to the mass of the free peptide  $[M + H]^+$  at  $m/z$  1253.6. In CID fragment spectra of copolymerized peptide, we identified three diagnostic fragment ions that were shifted by a multiple of 125 mass units according to the number of attached ECA subunits: (i) the b2-ion that represents the N-terminal fragment containing pyroglutamic acid and histidine, (ii) the a2-ion that represents a loss of carbon monoxide from the b2-ion and (iii) the histidine immonium ion that is an internal cleavage product containing the histidine side chain only. The modification of the histidine immonium ion in combination with the modification of b2- and a2-ions identifies the ECA subunits residing at the side chain of His2 of D-Lys<sup>6</sup>-GnRH. No other amino acid was found to be modified since all identified C-terminal fragments up to y8-ion were constant throughout all modified peptides.

Usually, the anionic polymerization of pure ECA subunits is initiated by hydroxyl ions present in the aqueous dispersed droplets, followed by a chain reaction.<sup>1</sup> Certain drugs however have also been reported to be able to initiate the reaction.<sup>28</sup> In the case of D-Lys<sup>6</sup>-GnRH, the unprotonated histidine side chain ( $pK_b$  7.96) with its electron-rich heterocycle may initiate the polymerization by a nucleophilic attack of an ECA monomer (Figure 6). The resulting positive charge of the nitrogen in position 3 of the imidazole structure can be delocalized, hence stabilized within the heterocycle. Restabilization of the aromatic ring may occur upon deprotonation of the nitrogen in position 1. The resulting negatively charged, hence activated, conjugate can then attack another monomer and continue the chain reaction. The reaction is terminated by protonation of the negatively charged carbon on the activated terminal ECA-subunit (Figure 6).

We found that termination occurs earlier in peptide copolymers compared to homogeneous PECA polymer, since polymer signals were still visible at  $m/z > 5000$  for empty PECA nanoparticles (Figure 2(a)) corresponding to  $>40$  ECA

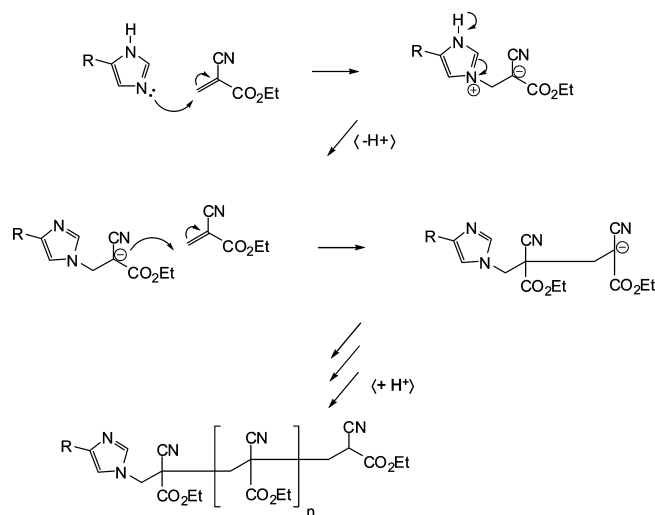


**Figure 6.** Suggested reaction mechanism of the nucleophile attack involving the histidine side chain of D-Lys<sup>6</sup>-GnRH as a reaction initiator. The polymeric chain reaction continues in an elongation reaction until the reaction is terminated either by the sterical hindrance of the growing bulky peptide substituent or a proton is transferred from the peptide, which is positively charged; CN = cyano side group, and Et = ethyl ester group.

subunits, while copolymerized particles (Figure 2(b)) only showed copolymer signals with peaks of reasonable threshold corresponding to  $<8$  ECA subunits. The strongest signals of peptide/ECA copolymer ranged from 2 to 4 conjugates of ECA subunits (Figure 2(b)) in comparison to 13-mers in homogeneous PECA nanoparticles (Figure 2(a)). The termination of polymerization of peptide/ECA copolymers is probably influenced by the close vicinity of the peptide either by a sterical hindrance and restricted accessibility of the activated terminal ECA subunit or more likely, by the transfer of a proton from the peptide itself that is positively charged ( $pI$  8.5) at neutral pH.

Mass spectrometric analysis of copolymerized D-Lys<sup>6</sup>-GnRH revealed clear evidence for a covalent interaction of peptide with ECA subunits, which might explain the observed low peptide release from the nanoparticles. Release studies under more physiological conditions confirmed the low release of D-Lys<sup>6</sup>-GnRH conducted in artificial gastric juice pH 1.2 (United States Pharmacopeia standards) (data not shown). However, it does not explain the presence of free peptide when the nanoparticles were dissolved after 5 days of incubation in water. We therefore expect the peptide to be entrapped and released by different mechanisms and/or molecular interactions. During the release study, fractions of free, mobile peptide were released from the nanoparticles and detected in the release medium. The HPLC peak used for the quantification of the amount of peptide released referred to the unmodified D-Lys<sup>6</sup>-GnRH species only and was confirmed with MALDI TOF MS (data not shown). Peaks referring to copolymers could not be identified using our HPLC method, which was optimized to specifically detect D-Lys<sup>6</sup>-GnRH. However, the bioerosion of nanoparticles as part of particle degradation is another possible

(28) Grangier, J. L.; Puygrenier, M.; Gautier, J. C.; Couvreur, P. Nanoparticles as Carriers for Growth-Hormone Releasing-Factor. *J. Controlled Release* **1991**, *15*, 3–13.



mechanism for a slow release of drug from the nanoparticles. Bioerosion has been suggested for a copolymerized system consisting of growth hormone releasing factor (GHRH), a 44-amino acid peptide hormone, and PECA nanoparticles.<sup>28</sup> This could involve both the release of free peptide from copolymer and the release of smaller fractions of copolymer provided they are soluble in the release medium. Figure 2(c) shows signals corresponding to non-peptide-associated polymer, which were not detected in the peptide/ECA copolymer initial mass spectra (Figure 2(b)), which could be explained by the bioerosion of copolymer. Peptide released, either as free peptide or peptide/ECA copolymer, will leave the nanoparticle with a negative charge, which in return can electrostatically attract free peptide present in solution. This would explain both the presence of free D-Lys<sup>6</sup>-GnRH in the mass spectrum and the low signal intensities of the smaller peptide/ECA copolymers after 5 days of release (Figure 2(c)). Conclusively, the overall low level of free peptide quantifiable in the release medium could be a result of (a) the HPLC assay not detecting the released peptide/ECA copolymer fractions and (b) peptide released from the nanoparticle reabsorbing onto the particle surface.

Pitaksuteepong et al.<sup>16</sup> reported that small, positively charged molecules ( $M_w < 1000$  Da) yield the highest entrapment rates in PECA nanoparticles. This was explained by electrostatic interactions between the negatively charged particles (zeta potential of empty particles  $-20$  mV) and positively charged molecules. D-Lys<sup>6</sup>-GnRH ( $pI$  8.5) is also positively charged at neutral pH. Charges are located mainly among the arginine ( $pK_b$  1.51) and the lysine residues ( $pK_b$  3.46). We observed adsorption of peptide onto preformed empty PECA particles as indicated by the presence of free peptide in the mass spectra of dissolved nanoparticles (Figure 4). Since nanoparticles were washed thoroughly prior to MALDI MS, the association of free peptide with PECA polymer must be relatively strong and is possibly due to molecular interactions including electrostatic interactions. Additionally, a small amount of the adsorbed peptide was present as peptide/ECA copolymers demonstrating copolymerization after adsorption. HPLC analysis of the supernatants suggested the fraction of peptide associated with the

nanoparticles via adsorption to be rather small (about 9%) and the overall surface charge of the nanoparticle was not affected significantly ( $P > 0.05$ ). Association may have occurred due to both electrostatic interactions and copolymerization of the peptide. Copolymerization can only occur when free ECA monomers become available and activated. Based on their study with PBCA nanoparticles, Ryan and McCann<sup>15</sup> have suggested an unzipping depolymerization/repolymerization mechanism as part of a base catalyzed polymer degradation, yielding reactive species accessible for further nucleophilic attack. Our findings of peptide copolymerization with preformed PECA nanoparticles support this theory. Histidine in general has weak basic characteristics ( $pK_b$  7.96) and more importantly strong nucleophilic properties, which may provoke the repolymerization with depolymerized ECA monomers. A depolymerization/repolymerization mechanism may also contribute to the overall slow release of D-Lys<sup>6</sup>-GnRH.

## 5. Conclusions

Using MALDI tandem time-of-flight mass spectrometry we have shown that His2 of D-Lys<sup>6</sup>-GnRH covalently interacts with ECA subunits during *in situ* polymerization and when *ex situ* added to preformed PECA nanoparticles. The quantity of the copolymerized fraction is yet to be determined. However, the potential reactivity of histidines toward poly(ethylcyanoacrylates) both *in situ* and *ex situ* needs to be considered when using such polymeric delivery systems, since the covalent interaction may alter nanoparticle characteristics such as surface charge, entrapment efficiency and release profile substantially.

**Acknowledgment.** The study was funded by FRST (Foundation for Research, Science and Technology) New Zealand. Acknowledgement is given to Mr. David Schmierer, School of Pharmacy, University of Otago and Dr. Dave Larsen, Chemistry Department, University of Otago, for valuable discussion.

MP900043E